Texture, twinning and metastable "tetragonal" phase in ultrathin films of HfO_2 on a Si substrate

I. MacLaren[a,z] , T. Ras[a], M. MacKenzie[a], A.J. Craven[a], D.W. McComb[b], S. De Gendt[c,d],

[a]*Department of Physics and Astronomy, Faculty of Physical Sciences, University of Glasgow, Glasgow G12 8QQ, UK*

[b]*Department of Materials, Imperial College London, London SW7 2AZ, UK*

[c]*IMEC, B-3001 Leuven, Belgium*

[d]*Department of Chemistry, K. U. Leuven, B-3001 Leuven, Belgium*

[z] E-mail: i.maclaren@physics.gla.ac.uk

Abstract

Thin HfO_2 films grown on the lightly oxidised surface of (100) Si wafers have been examined using dark-field transmission electron microscopy and selected area electron diffraction in plan view. The polycrystalline film has a grain size of the order of 100 nm and many of the grains show evidence of twinning on (110) and (001) planes. Diffraction studies showed that the film had a strong [110] out-of-plane texture, and that a tiny volume fraction of a metastable (possibly tetragonal) phase was retained. The reasons for the texture, twinning and the retention of the metastable phase are discussed.

Introduction

It is well known that replacements to Si(O,N) – based dielectrics need to be found to enable further miniaturisation of MOSFETs and HfO_2-based materials have already been demonstrated for this application by major manufacturers. Whilst an amorphous film would be ideal, in reality, such HfO_2 films will always crystallise during the rapid thermal annealing processes applied to silicon wafers and thus it is important to understand the structures formed in the crystallisation of these films since they may well influence the properties[1-5]. The present work investigates crystallographic texture in such films, how this results in the frequent appearance of multiple twinning in the films, together with evidence for the retention of a small fraction of some metastable tetragonal/cubic/orthorhombic phase in the films. The reasons for the twinning are discussed and simple models are presented to explain the texture and the resultant twinning in the films.

Experimental

(100) Si wafers were prepared by cleaning with dilute HF, oxidising with an O_3/deionised water solution to form 1.0 nm of native SiO_2. HfO_2 was then deposited using 80 cycles of atomic layer deposition (ALD) using $HfCl_4/H_2O$ at 300°C to produce a target film thickness of 3.5-4.0 nm. Cross sectional studies of films prepared in the same way show thicknesses of about 3.5 nm[6]. The wafers were then subjected to a post-deposition furnace anneal under an O_2 atmosphere at 500°C for 1 minute resulting in crystallisation to polycrystalline HfO_2 (loaded at 400°C, heated to 500°C in about 30s, held for 1 minute, and cooled again to 400°C in about 1 minute, followed by further cooling under N_2). Some samples were prepared using further deposition of amorphous-Si onto the HfO_2 film followed by annealing to produce a

poly-Si gate, but very similar results were seen to those for bare HfO_2 films and only these bare annealed HfO_2 films without the rest of the gate stack deposited on top will be discussed in this paper.

Preparation of plan-view TEM specimens was performed using conventional techniques of grinding, cutting 3 mm discs, polishing, dimpling and finally ion-milling to perforation. All material removal was performed from the substrate side to leave the HfO_2 film intact and easily visible close to the hole, but all regions examined had some supporting Si substrate remaining below the ultrathin HfO_2 film. Investigations of the nanoscale structure were performed using conventional dark-field imaging (to allow imaging of the film alone without the strong diffraction contrast of the silicon substrate) combined with selected area diffraction using FEI Tecnai TF20 and T20 transmission electron microscopes (FEI Corp., Eindhoven, The Netherlands); images and diffraction patterns were recorded either using conventional negative film, a Gatan MSC Camera (Gatan Inc., Pleasanton, CA) or an Olympus SIS Megaview III CCD camera (Olympus SIS GmbH, Garching, Germany). Diffraction patterns were modelled using Desktop Microscopist (Lacuna Laboratories, formerly of Beaverton, OR).

Note on structures and twinning in HfO_2

HfO_2 is known to display monoclinic, tetragonal and cubic structures at ambient pressure, analogous to the well-known fluorite or fluorite-derived structures in ZrO_2[7]; additionally two orthorhombic modifications are known to exist under high pressure conditions[8]. At temperatures lower than 1800°C the stable structure is monoclinic with lattice parameters of a ~ 5.12 Å, b ~ 5.17 Å, c ~ 5.29 Å and β ~ 99.2° (space group $P2_1/c$); this structure is well studied and numerous refinements exist[7,8,10].

At temperatures of 1800-2400°C, however, it takes the form of a tetragonally distorted fluorite structure, analogous to tetragonal zirconia (space group $P4_2/nmc$)[7]. Unfortunately, the tetragonal structure is less well studied and fewer refined structures are available, so calculating the structure is most easily performed by using atom positions refined for tetragonal ZrO_2 (see for example Teufer[11]) together with cell parameters determined for HfO_2[7]. For simplicity of comparing the phases, the tetragonal phase is expressed in terms of the face-centred cell used by Wang *et al.*[7] in his comparison tables rather than the primitive cell, and parameters of a ≈ 5.15 Å and c ≈ 5.29 Å were given for the face-centred cell (measured at ~1800 °C).

Although the monoclinic phase is the thermodynamically stable phase at room temperature, there have been numerous reports of metastable phases existing in thin films or nanoparticles of HfO_2 including of tetragonal, cubic and orthorhombic phases[2,4,12-15]. In most cases, it was difficult to unambiguously determine which of these phases was present since the main diffraction peak common to all these phases lies at a similar d-spacing around 2.90-2.95 Å (which indexes as 111_{cubic}, $111_{face\text{-}centred\text{-}tetragonal}$ or $211_{orthorhombic}$) and sits between the $11\bar{1}_{monoclinic}$ and $111_{monoclinic}$ diffraction rings at d spacings of ~ 3.15 Å and 2.82 Å, respectively. For simplicity in performing the calculations done in this paper, we assume that the metastable phase was tetragonal in accordance with Triyoso *et al.*[2], but it was not possible to unambiguously determine its structure using electron diffraction for the reasons noted later.

Twinning occurs in a crystal where the stacking of atomic planes changes order or direction at a specific plane, the twin is formally described by a mirror operation on this plane or a 2-fold rotation perpendicular to this plane. Twinning can occur in a structure as a consequence of a phase transformation when a mirror

symmetry plane of the parent structure is lost as a consequence of the transformation; this lost mirror plane can become a twin plane in the low symmetry structure. (The reader is referred to a wider discussion of the formation of domain boundaries due to symmetry reduction in phase transformations by Van Tendeloo and Amelinckx[16]). When HfO_2 (or ZrO_2) transforms from the high symmetry cubic or tetragonal phase into the low symmetry monoclinic phase some mirror or mirror-glide elements are lost. The $P4_2/nmc$ tetragonal structure contains mirror planes on (100)/(010), (001) together with mirror-glide planes on $(110)/(1\bar{1}0)$. The only one retained in any form by the $P2_1/c$ monoclinic structure is a c-glide plane on $(010)_{monoclinic}$. Assuming that the tetragonal-monoclinic transformation happens with [001] parallel in both phases (since this axis is much longer than the other axes in either structure), and with [110] of the primitive tetragonal becoming [100] of the monoclinic phase, then the lost mirror planes expressed in the monoclinic indices will be (100), $(110)/(1\bar{1}0)$ and (001). These will become possible twin planes of the structure and all of these twinning modes have previously been observed in ZrO_2 and/or HfO_2[12,17,18]

Results and Analysis

A typical dark-field image of the structure in the specimen is shown in Fig. 1 (using an objective aperture placed to exclude all contributions from the silicon substrate but to allow several different HfO_2 reflections including the 111, $11\bar{1}$ and 110/011 rings labelled in Figure 2a to contribute to the image). This clearly shows the polycrystalline nature of the film and it is also clear that most grains appear to be in the size range of 50 – 200 nm, which accords well with previous observations by plan view TEM at IMEC[19] and using AFM by Triyoso *et al.*[2]. Please note that such plan-view grain size estimations are likely to be more representative than those made using

many other methods including cross-sectional TEM where the irregular shape of grains may give misleading results[20] or by X-ray Scherrer broadening, where internal twinning of the monoclinic phase may just give a measurement of the size of the internal twins. Many grains are also found with a striped appearance and these are investigated further below. Selected area diffraction from such large areas gives ring patterns as shown on the left hand half of Figure 2 (slightly tilted away from the substrate [001] normal direction to reduce the intensity of the silicon diffraction spots). Since silicon reflections are always found superimposed on the diffraction patterns, the ring patterns from the HfO_2 film could be accurately calibrated and the plane spacings mainly accord with the monoclinic crystal structure, which is normally stable at room temperature. Nevertheless, several spots are observed in a ring between the $11\bar{1}$ and 111 rings (see the inset in Fig. 2); these cannot arise from the monoclinic phase and correspond, rather, to a reflection from one of the other forms of HfO_2 (111_{cubic}, $111_{\text{tetragonal}}$ and $211_{\text{orthorhombic}}$). Thus, a small volume fraction of the metastable phase is clearly present in the film, but the number of these spots compared to $11\bar{1}$/111 reflections from the monoclinic phase is so small that it seems unlikely that there is even a 1% volume fraction of metastable phase remaining. The right hand half of Figure 2 shows a selected area diffraction pattern of the same area with the sample tilted to an angle of 45° away from the substrate normal. Comparing this with the zero tilt diffraction pattern, a number of observations are clear. Along the tilt axis, little change has occurred, as one would expect. However, perpendicular to this axis, the $11\bar{1}$ and 111 rings are weakened and the 200/020/002 ring just outside these is significantly more intense (even if the reflections in this ring are rather diffuse and not well separated due to the tiny thickness of the film); the consequences of this for film texturing will be discussed in section III.

Figure 3a shows a higher magnification dark-field image of one striped grain, using a dark-field tilt such that only spot *a* from the closely spaced pair of spots *a* and *b* in the selected area diffraction pattern of Figure 3c contributes to the image. Similarly, Figure 3b was formed using a dark-field tilt such that only spot *b* from the pair contributes to the image. Thus, it is clear that the stripe contrast comes from a pair of closely spaced diffraction spots, probably arising from twinning. Similarly, closely-spaced diffraction spots were found in all cases where striped grains were investigated in detail. Based on their lattice spacing these closely spaced spots in Figure 3c could be identified as either 022 (d = 1.838 Å) or $21\bar{2}$ (d = 1.851 Å) type reflections. The angle between the spots, together with the angle of these spots in the diffraction pattern to the twin plane in the image (after compensation for the rotation of the diffraction pattern with respect to the image), were used to identify the twin relationship by comparison with simulations. Diffraction patterns were simulated for (100), (001) and (110) twin relationships, but only (110) twinning could explain the diffraction pattern; a modelled diffraction pattern is shown in Figure 3d. It may be noted that bright diffraction contrast only occurs over a limited area of the grain in either of Figs 3a or 3b due to specimen bending, as is often the case in thin TEM specimens.

Figure 4a shows a dark-field image of a grain showing stripe patterns in two orthogonal directions. A selected area diffraction pattern from this grain is shown in Figure 4b. Since the distortion from face-centred-cubic (FCC) is still relatively small, this pattern still resembles a <110> FCC diffraction pattern, but having a cross shape of four separate reflections at each {111} position. Also for the reflections from {002} planes (top and bottom) there is an arc of three reflections. Modelling of the effect of the different twinning modes on the [110] diffraction show that $(1\bar{1}0)$ twinning

would produce a spot splitting of the {111} spots in a horizontal direction. In contrast to this, (100) and (001) twinning cause splitting of {111} spots in the vertical direction. Thus, the diffraction pattern shows that two twinning modes are involved and modelling diffraction patterns shows a better match for a combination of (110) twinning and (001) twinning in the same grain. This is illustrated in the modelled diffraction pattern of Figure 4c where the red and blue triangles (horizontal splitting) represent contributions from the (110) twinning and the green and brown squares (vertical splitting) show contributions from the (001) twinning. This type of multiple twinning resulting in cross shaped spots on [110] diffraction patterns seems to be a common feature of the films and has frequently been observed in the different specimens studied in this project.

Figure 5a shows a selected area diffraction pattern from one grain where a $111_{metastable}$ spot is observed between the 111_{m} and $11\bar{1}_{m}$ spots from a grain that has undergone (001) twinning. A variety of dark field images were then formed with different tilts of the beam with respect to the objective aperture in order to create images from specific diffraction spots only. Note that the spots were very closely spaced so that it would be impossible to just form an image with the $111_{metastable}$ spot alone. Three images of these images were then combined to form a three-colour RGB image as follows:

i) The $111_{monoclinic}$ and $111_{metastable}$ spots – red channel

ii) The $11\bar{1}_{monoclinic}$ and $111_{metastable}$ spots – green channel

iii) The $11\bar{1}_{monoclinic}$ spot alone – blue channel

The results are shown in Figure 5b and areas just showing red or showing a green-blue mix (cyan) must be monoclinic (and this highlights the twinning very well), but the area at the top of the grain showing a red-green mix can only be diffracting into

the $111_{metastable}$ spot and is thus confirmed as the metastable phase. Solid colour areas in blue and red to the lower right are monoclinic. Please note it was not possible to directly determine the structure of the metastable phase using diffraction since extended exposure to an intense electron beam often resulted in the transformation to the monoclinic phase (probably as a consequence of local heating or electron beam induced mobility).

Discussion

At low tilts from the substrate normal there is strong diffracted intensity for 111 and $11\bar{1}$ type reflections, together with some significant intensity on 110/011 and 220/022 reflections, as shown in Figures 2a and 4b. When the sample is tilted to ~ 45° off-axis the 111 and $11\bar{1}$ are weakened whereas the 200/020/002 ring is strengthened (from being almost invisible at low tilts). This suggests an average film texture in which many {111} and $\{11\bar{1}\}$ planes lie perpendicular to the film plane, but that there are a lot of (200)/(020)/(002) planes lying at 45° to the film plane. If the pattern of Fig. 4b was in any way representative, and this pattern was frequently observed at different locations and in different samples, then the out of plane direction is [110]. This would also explain the strength of the 111 and $11\bar{1}$ rings at low tilts, as well as the relative weakness of the 200/020/002 rings since the 200 and 020 reciprocal lattice directions will lie out of plane and only 002 will lie in plane. Now since the monoclinic cell of hafnia is a basically a distorted cubic cell, if the [110] direction lies out of plane, then the (200) and (020) planes will lie at approximately 45° to the plane, which would explain the increased diffracted intensity to the 200/020 ring at such tilts. Thus, there is strong evidence from the diffraction data that the film shows a clear [110] out-of-plane texture. This observation accords well with that

of Bohra *et al.*[4] who also noted a [110] out-of-plane texture in 2 nm HfO_2 films that displayed a metastable orthorhombic or cubic phase.

It should be noted that the texture is a clear out-of-plane texture and there is no in-plane texture, as would be expected since the HfO_2 is not epitaxially grown on the Si but grows on a thin layer of chemically grown amorphous SiO_2 (as may for instance be seen in previous publications on HfO_2 gate oxides[21]). The key question is why the [110] texture appears on crystallisation during the post-deposition anneal and this may be answered by considering its growth. Previous studies of particulate HfO_2 growth have found that it typically transforms from amorphous to the tetragonal phase before this transforms to the stable monoclinic low-temperature phase[12] whereas thin film studies have variously claimed to have found metastable cubic, tetragonal or orthorhombic phases forming either prior to the stable monoclinic phase, or retained as a minority phase alongside the monoclinic phase[4,13-15]. If we consider the structure of tetragonal or cubic HfO_2 then there is only one low index plane in the structure that is uncorrugated and charge neutral: the {110} plane, and this is illustrated in Figure 6. So, it would seem likely that a metastable cubic/tetragonal/orthorhombic phase is formed in the initial crystallisation where rafts of {110} planes form starting from the SiO_x interface, thus seeding a [110] texture. It should be noted that Bohra *et al*. also noted a <110> out of plane texture in their metastable phase films[4].

This [110] texture inevitably leads to twinning on transformation to the monoclinic phase for very simple reasons. Figure 7 shows a schematic diagram of the effect of the transformation on a single grain of tetragonal hafnia. It is clear that the transformation will lead to significant shear stresses (as well as delamination stresses at the film substrate interface) due to the change in cell angles, but if the

transformation direction is periodically reversed as in Figure 7c, then these can be minimised at the expense of twinning the grain.

In some cases, however, two twinning modes are observed in the same grain perpendicular to each other with both {110} and (001) twinning. The reason for this is most likely related to the overall shape strain caused by twinning after transformation from the metastable phase (assumed for these calculations to be tetragonal). Unfortunately, we do not have access to any lattice parameters for tetragonal HfO_2 near room temperature. To get round this difficulty we have extrapolated some room temperature lattice parameters for tetragonal zirconia from the data provided by Wang et al.[7] in their graph of the variation of lattice parameters with temperature for the tetragonal and monoclinic phases (Figure 4a in their paper). The extrapolated lattice parameters for the tetragonal phase at room temperature were a = 5.061 Å and c = 5.201 Å. Although there is some uncertainty about the extrapolation of the tetragonal parameters comparison to this lattice parameters for nanoparticles of metastable tetragonal zirconia at room temperature show parameters of a = 5.065 Å and c = 5.1685 Å[22], so these hafnia extrapolations seem reasonable.

If we consider a grain oriented with [110] out-of-plane, and it twins on $(1\bar{1}0)$ planes, then perpendicular to the twin plane, the spacing will change by about +0.95 % on transformation. The perpendicular in-plane direction will correspond to [001] and this will increase in length by about +1.7 % on transformation. Thus {110} twinning causes an anisotropic lengthening of the grain along [001].

If we twin the same grain on (001), then the strain along the direction perpendicular to these (001) planes is only ~ +0.42 %, which is significantly less than that caused by the $(1\bar{1}0)$ twinning in the [001] direction. In the perpendicular $[1\bar{1}0]$

direction, (001) twinning causes a large strain of ~ +1.7 %. So, (001) twinning causes an anisotropic expansion in the $[1\bar{1}0]$ direction.

The consequence of the anisotropic shape strain for both {110} and (001) twinning is that to keep the grain expansion as isotropic as possible we will need to have a combination of {110} and (001) twinning in the same grain, and this is illustrated in Figure 8. This has features in common with earlier suppositions by Zhao *et al.*[19] that twinning may run in perpendicular directions but this now has a proper crystallographic analysis and a strain-based justification for why perpendicular twinning in a single grain takes place.

Finally, it remains to consider why a small fraction of metastable material remains in the film as seen in diffraction patterns and imaged in Figure 5b. It is well known that a certain fraction of the tetragonal phase can be metastably retained to room temperature in zirconia due to physical constraints in the sample preventing the transformation; and this is of great technological importance in transformation-toughened zirconia[23]. In view of the much smaller volume change in the tetragonal to monoclinic transformation for HfO_2, transformation-toughening cannot be usefully applied to this material[7]. Nevertheless, it is believable that a small volume fraction of the tetragonal phase or possibly one of the other metastable phases could be retained to room temperature in areas where the compressive stress is so high that the transformation to monoclinic is inhibited. Previous studies have also found diffraction evidence for the retention of a small fraction of tetragonal/cubic/orthorhombic material in monoclinic HfO_2 films[18,21].

Conclusions

Thin (3.5-4 nm) films of HfO_2 grown by ALD on a silicon (100) substrate with 1 nm chemically produced oxide on the surface show a clear polycrystalline structure with a grain size of the order of 100 nm. Electron diffraction reveals that there is a notable [110] out-of-plane crystallographic texture in these films. The grains often display twinning with some grains showing (110) twinning, whereas others show both (110) and (001) twinning. A tiny volume fraction of metastable tetragonal/cubic/orthorhombic material could also be detected in the films.

The out-of-plane texture probably arises from the film initially crystallising in a tetragonal, cubic or possibly orthorhombic structure with rafts of atoms on (110) planes forming parallel to the substrate, followed by the transformation to monoclinic. The transformation to monoclinic also drives the twinning since this will minimise shear strains. It is shown that two perpendicular twinning modes help to equalise the overall shape strain and this may explain the observation of multiple twinning in some larger grains. The strain resulting from the transformation may also be high enough to prevent the transformation of some small areas to the monoclinic phase resulting in the retention of a small volume fraction of the metastable phase. This retention of the metastable phase may be significant for its use as a high-k layer since the tetragonal phase is known to have a higher dielectric constant than the monoclinic phase[3]. This could lead to local inhomogeneities in dielectric constant and thus in the electric field applied to the channel beneath the gate in a MOSFET device.

Acknowledgements

Parts of this work were performed under the auspices of the EPSRC research grant GR/S44280/01 (Chemistry, Structure and Bonding in High-k Gate Oxide

Stacks). Mr Tadeus Ras contributed to this work as part of an ERASMUS exchange to the University of Glasgow from the Johannes Gutenberg-Universität Mainz, Germany. The authors also acknowledge the contribution of Miss Stephanie Craigens to the initial stages of this work as part of her final year BSc project. This work would not have been possible without specimen preparation by Mr Brian Miller or technical assistance with the microscopes from Dr Sam McFadzean and Mr Colin How.

Figure captions

FIG. 1: Large area dark field micrograph of the HfO_2 film showing grains of the order of 100 nm in size, which often show a striped or striated appearance.

FIG. 2: Selected area diffraction patterns from the film: left hand half recorded at 5° tilt from the [001] axis of the Si substrate so as to be almost on axis, but with reduced diffracted intensity from the Si; right hand half recorded at 45° tilt from the [001] axis of the Si.

FIG. 3: More detailed analysis of a striated grain: a) dark field image created using one diffraction spot (labelled **a** in Figure 3c)); b) dark field image created using the diffraction spot **b** of Figure 3c); in both a) and b) an asterisk is inserted to the same position to show that the contrast in a) is from a different set of lamellae to that in b); c) selected area diffraction pattern of this area with some spots labelled and the boundary trace drawn in, after compensating for the rotation between diffraction and image modes; d) modelled diffraction pattern created using Desktop Microscopist assuming that the spots **a** and **b** come from crystals related by (110) twinning.

FIG. 4: Detailed analysis of a grain with striations in two perpendicular directions: a) dark field image; b) selected area diffraction pattern showing splitting into four spots in a cross shape at the $111/11\bar{1}$ positions; c) modelled diffraction pattern created using Desktop Microscopist using both (110) twinning (red, blue triangles) and (001) twinning (dark brown, dark green squares), colour and shapes were added to help the reader.

FIG. 5: Imaging of the metastable phase in a grain in the film: a) Diffraction pattern from the area of interest with spots labelled, the metastable spot is indexed according to the face-centred-tetragonal/cubic unit cell; b) Three colour image showing twinned monoclinic HfO_2 in red and cyan, together with the untwinned metastable phase at the top in a greenish/red colour.

FIG. 6: The (110) plane of the face-centred-tetragonal HfO_2 structure (almost identical to the same plane in the face-centred-cubic structure).

FIG. 7: Schematic diagram of how twinning minimises the shear deformation of a single grain: a) tetragonal parent grain; b) untwinned monoclinic grain with a large shear deformation; c) twinned monoclinic grain with a similar shape to the parent grain.

FIG. 8: Schematic diagram of how twinning on two planes minimises anisotropic shape strain of a grain.

References

1. C. Wiemer, S. Ferrari, M. Fanciulli, G. Pavia, and L. Lutterotti, *Thin Solid Films*, **450**, 134 (2004).
2. D. H. Triyoso, R. I. Hegde, B. E. White, and P. J. Tobin, *J. Appl. Phys*., **97**, 124107 (2005).
3. R. I. Hegde, D. H. Triyoso, S. B. Samavedam, and B. E. White, *J. Appl. Phys*., **101**, 074113 (2007).
4. F. Bohra, B. Jiang, and J. M. Zuo, *Appl. Phys. Lett*., **90**, 161917 (2007).
5. E. E. Hoppe, R. S. Sorbello, and C. R. Aita, *J. Appl. Phys*., **101**, 123534 (2007).
6. A. J. Craven, M. MacKenzie, D. W. McComb, and F.T. Docherty, *Microelectron. Eng.*, **80**, 90 (2005).
7. J. Wang, H. P. Li, and R. Stevens, *J. Mater. Sci*., **27**, 5397 (1992).
8. J. Kang, E. C. Lee, and K. J. Chang, *Phys. Rev. B*, **68**, (2003).
9. R. Ruh and P. W. Corfield, *J. Am. Ceram. Soc*., **53**, 126 (1970).
10. D. M. Adams, S. Leonard, D. R. Russell, and R. J. Cernik, *J. Phys. Chem. Solids*, **52**, 1181 (1991).
11. G. Teufer, Acta Cryst., **15**, 1187 (1962).
12. J. Tang, T. Zhang, P. Zoogman, J. Tabbri, S. W. Chan, Y. M. Zhu, L. E. Brus, and M. L. Steigerwald, *Adv. Funct. Mater*., **15**, 1595 (2005).
13. I. A. El-Shanshoury, V. A. Rudenko, and I. A. Ibrahim, *J. Am. Ceram. Soc*., **53**, 264 (1970).
14. M. Ritala, M. Leskela, L. Niinisto, T. Prohaska, G. Friedbacher, and M. Grasserbauer, *Thin Solid Films*, **250**, 72 (1994).

15. J. Aarik, A. Aidla, H. Mändar, V. Sammelselg, and T. Uustare, *J. Cryst. Growth*, **220**, 105 (2000).

16. G. Van Tendeloo and S. Amelinckx, *Acta Cryst*., **A30**, 431 (1974).

17. Z. Q. Shen, L. L. He, J. F. He, H. M. Cheng, and D. X. Li, *Nanotechnology*, **17**, 1207 (2006).

18. N. K. Simha, *J. Mech. Phys. Solids*, **45**, 261 (1997).

19. C. Zhao, V. Cosnier, P.J. Chen, O. Richard, G. Roebben, J. Maes, S. Van Elshocht, H. Bender, E. Young, O. Van Der Biest, M. Caymax, W. Vandervorst, S. De Gendt, and M. Heyns, *Mat. Res. Soc. Symp. Proc.*, **745**, N1.5.1 (2003).

20. A. J. Craven, M. MacKenzie, D. W. McComb, and F. T. Docherty, *Microelectron. Eng.*, **80**, 90 (2005).

21. M. MacKenzie, A. J. Craven, D. W. McComb, and S. De Gendt, *Appl. Phys. Lett*., **88**, 192112 (2006).

22. P. Bouvier, E. Djurado, C. Ritter, A. J. Dianoux, and G. Lucazeau, *Int. J. Inorg. Mater*., **3**, 647 (2001).

23. D. L. Porter, A. G. Evans, and A. H. Heuer, *Acta Metall*., **27**, 1649 (1979).

Figure 1

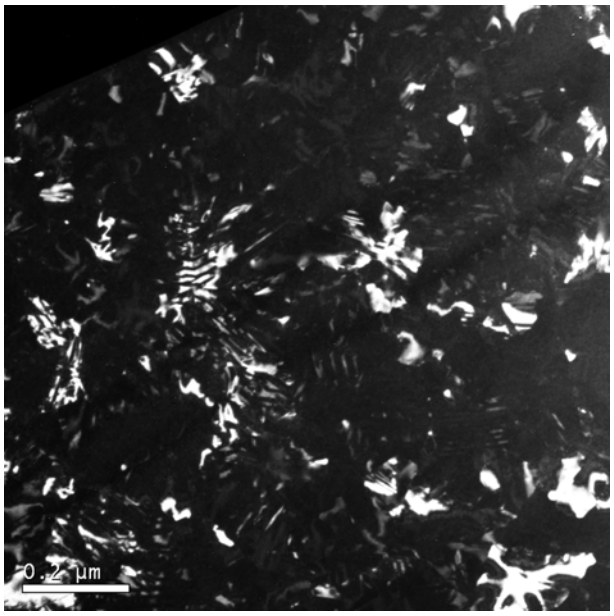

Figure 2

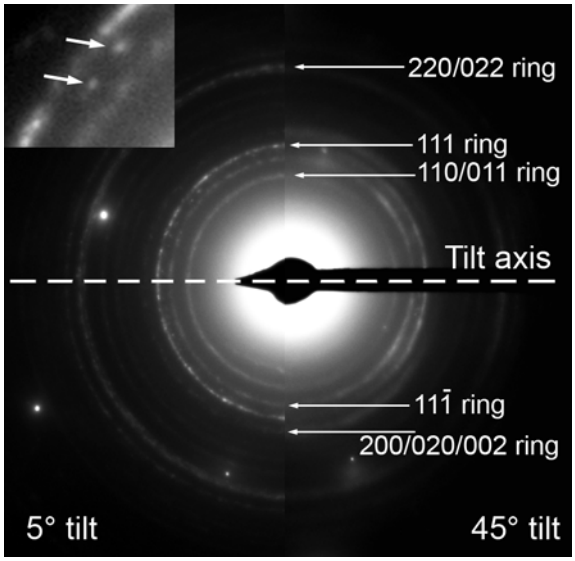

Figure 3

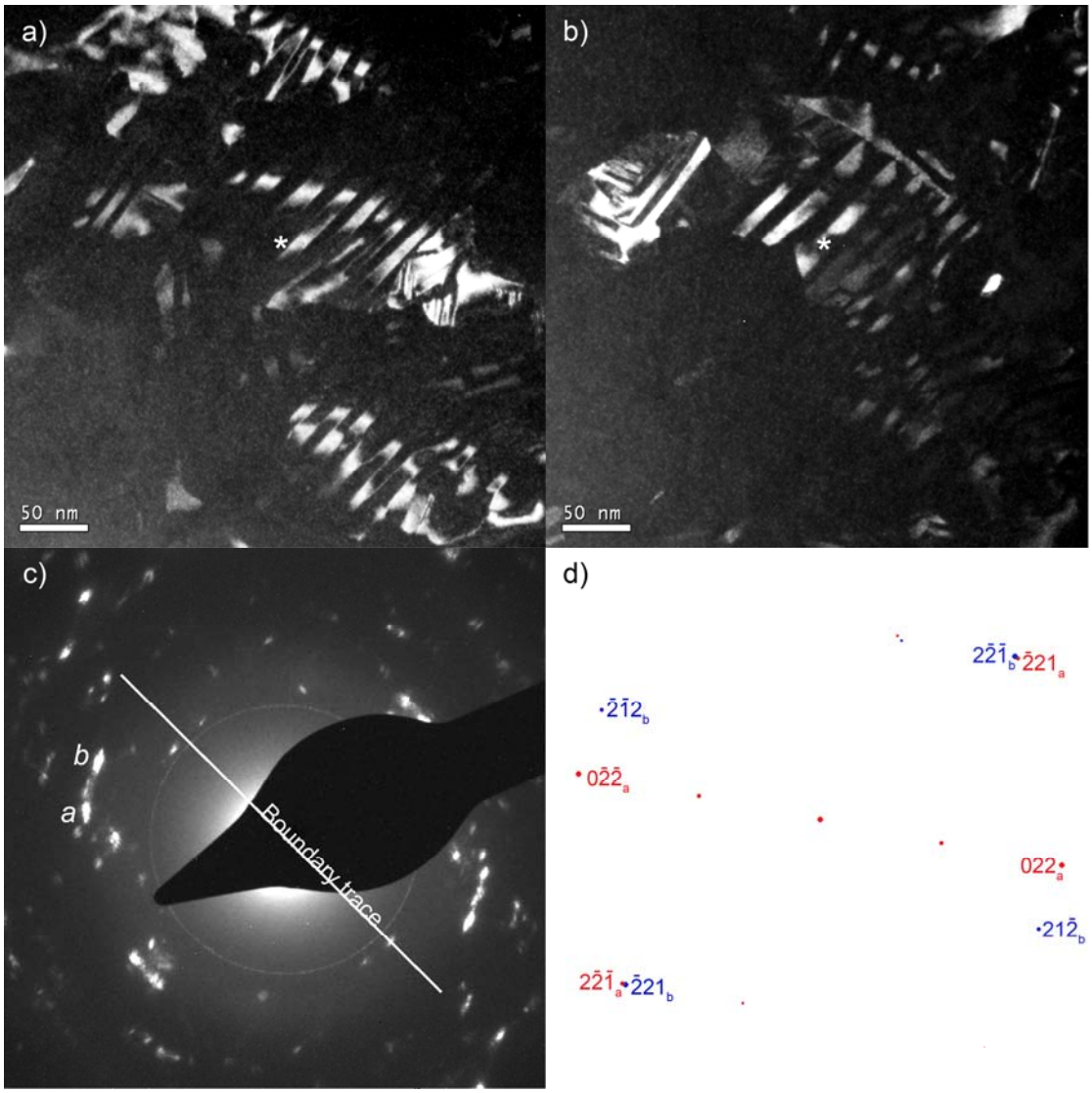

Figure 4

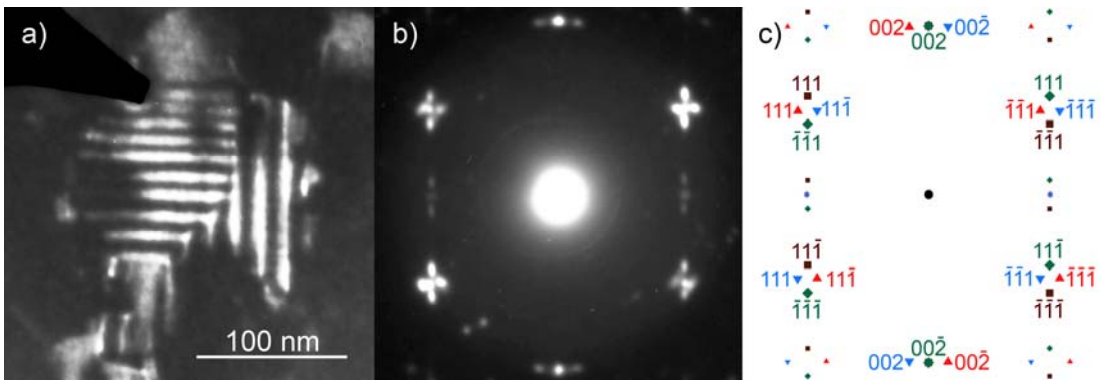

Figure 5

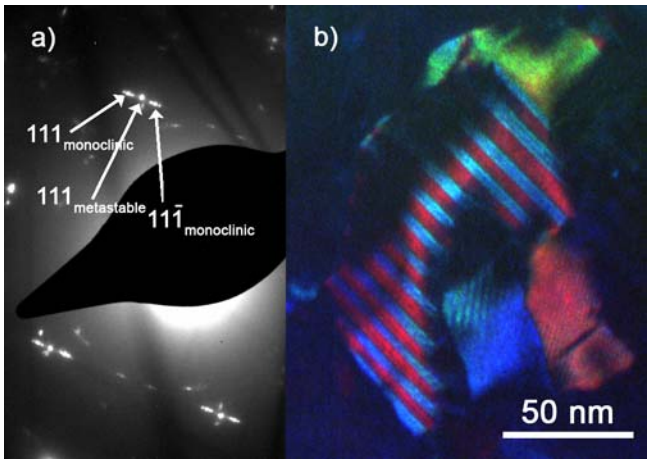

Figure 6

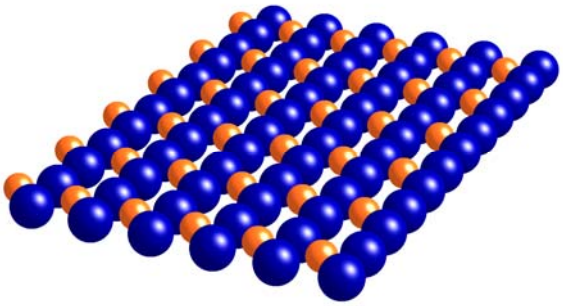

Figure 7

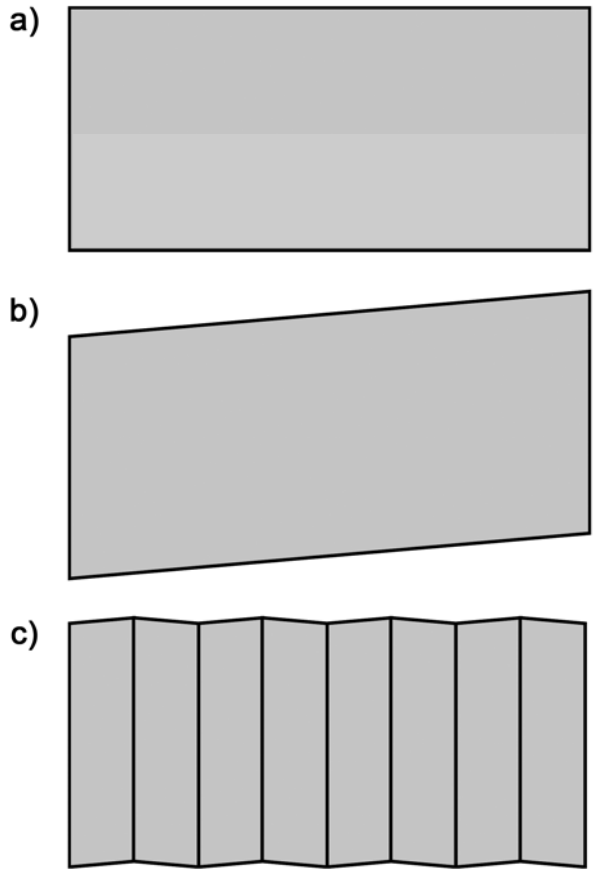

Figure 8